Dislocation structure of GaN films grown on planar and nano-patterned sapphire

Wanjun Cao, Jeffrey M. Biser, Yik-Khoon Ee, Xiao-Hang Li, Nelson Tansu et al.

Related Articles

Interfaces between nonpolar and semipolar III-nitride semiconductor orientations: Structure and defects
J. Appl. Phys. 111, 033507 (2012)

How do InAs quantum dots relax when the InAs growth thickness exceeds the dislocation-induced critical thickness?
J. Appl. Phys. 111, 013709 (2012)

Observation of non-basal slip in semipolar InxGa1-xN/GaN heterostructures
Appl. Phys. Lett. 99, 251909 (2011)

Characterization of GaSb/GaAs interfacial misfit arrays using x-ray diffraction
Appl. Phys. Lett. 99, 231906 (2011)

Response to "Comment on 'The effects of Si doping on dislocation movement and tensile stress in GaN films'" [J. Appl. Phys. 109, 073509 (2011)]
J. Appl. Phys. 110, 096102 (2011)

Additional information on J. Appl. Phys.

Journal Homepage: http://jap.aip.org/

Journal Information: http://jap.aip.org/about/about_the_journal

Top downloads: http://jap.aip.org/features/most_downloaded

Information for Authors: http://jap.aip.org/authors

Dislocation structure of GaN films grown on planar and nano-patterned sapphire

Wanjun Cao,[1,a] Jeffrey M. Biser,[1] Yik-Khoon Ee,[2] Xiao-Hang Li,[2] Nelson Tansu,[2] Helen M. Chan,[1] and Richard P. Vinci[1,a]

[1]*Department of Materials Science and Engineering, Center for Advanced Materials and Nanotechnology, Lehigh University, Bethlehem, Pennsylvania 18015, USA*
[2]*Center for Optical Technologies, Department of Electrical and Computer Engineering, Lehigh University, Bethlehem, Pennsylvania 18015, USA*

Plane view and cross-section transmission electron microscopy (TEM) images were used to compare the density, character, and curvature of dislocations developed during metalorganic vapor phase epitaxy (MOVPE) of GaN on planar c-plane sapphire with those developed during growth on nano-patterned c-plane sapphire. Scanning electron microscopy (SEM) characterization of GaN films at different stages of growth for both types of substrates complemented the TEM investigation. GaN growth on wafers patterned with an array of submicron sapphire bumps exhibited relatively uniform nucleation and initial growth, as well as early island coalescence. It is suggested that this coalescence results in a relatively small fraction of dislocations with partial screw character at the surface of the films grown on the patterned substrate, and that this may be responsible for the improvements in carrier lifetime and device efficiency seen in earlier studies on similar sapphire substrates. © 2011 American Institute of Physics. [doi:10.1063/1.3631823]

I. INTRODUCTION

Sapphire is commonly used as the substrate for III-Nitride light-emitting diodes (LEDs).[1] The efficiency of nitride LEDs can be enhanced by suppression of the non-radiative recombination rate and enhancement of the radiative recombination rate (R_{Rad}) in the quantum well (QW) active region.[2–4] Because of the ~16% lattice mismatch between sapphire and GaN, a high dislocation density in the range of $10^8 - 10^{10}$cm^{-2} (Ref. 1) is usually found in GaN epitaxial layers. The dislocations are generally accepted as detrimental to the emission and transport properties of GaN-based devices because they act as non-radiative electron-hole recombination centers.

To improve device efficiency through dislocation density reduction, several alternate growth methods have been adopted such as selective area growth (SAG) and epitaxial lateral overgrowth (ELO). Most of these methods favor a lateral 3D growth mode to relax the lattice mismatch between GaN and c-plane sapphire. However, the use of such techniques requires several processing steps, so a simple, effective alternative would be of value.

Conventional metalorganic vapor phase epitaxy (MOVPE) of GaN often involves a low-temperature (LT) GaN nucleation layer growth stage prior to the growth of the high-quality, high-temperature (HT) GaN layer.[5] In doing so, an etch back and recovery process has been found effective for improving HT GaN quality.[6,7] In this process, H_2 is used to etch back the LT GaN buffer layer so that intentional delay of island coalescence (recovery) can be achieved, and a high-quality thick GaN film may be grown.[8] Because the purpose of the etch-back process is to break down the LT GaN into micro-size islands, it is possible to avoid the etch-back and recovery processes by depositing on a sapphire substrate that has an array of submicron sapphire bumps on its surface.[6,7] It has been shown that this can lead not only to a reduction in processing time, but also to an increase in carrier recombination lifetime and device efficiency.[9] Although this improvement was initially attributed to a reduction in total dislocation density, this is not the only possible explanation.

II. EXPERIMENTAL

In this article, we present a comparison study of the dislocations in GaN films grown using MOVPE by the conventional method on polished c-plane sapphire (conventional GaN), and by an "'abbreviated growth mode" on nano-patterned c-plane sapphire (AGNP-GaN). When growing conventional GaN, a 30-nm-thick LT GaN (535 °C) buffer layer was first grown on the sapphire, followed by a standard H_2 etch-back process,[8] and finally HT GaN (1080 °C) recovery and growth. For AGNP-GaN samples, a square array of sapphire bumps was fabricated on the surface of a standard sapphire wafer using a novel process involving the oxidation and epitaxial conversion of Al islands.[10] The diameter of the submicron bumps was $200 - 300$ nm, and the thickness was ~100 nm; the pitch of the square array was about 1000 nm.[10] (Note that in early work on this patterning process,[10] a 10-nm-thick Al film was deposited prior to the e-beam lithography to enhance electrical conductivity of the substrate. This step has since been eliminated[6,7] by employing a variable pressure mode in the e-beam lithography process.) The GaN was grown on the patterned substrates using an abbreviated-growth-mode technique that consisted of a 15-nm-thick LT GaN buffer layer, followed *immediately* by HT GaN (without an intermediate etch-back and recovery process).

---

a)Electronic addresses: wac207@Lehigh.Edu, vinci@Lehigh.Edu.

110, 053505-1

For both fabrication methods (conventional and AGNP), the early-stage morphology of the GaN was examined after only 3 min of HT GaN growth using scanning electron microscopy (SEM) (Hitachi 4300SE/N). In addition, plane view and cross-section transmission electron microscopy (TEM) were used to characterize the dislocation character, inclination, and overall density in GaN films for which the thickness was approximately 4 μm (JEOL 2000FX, 200 kV accelerating voltage). Cross-section TEM samples were prepared by focused ion beam (FIB) milling, and plane view specimens were prepared by mechanical polishing and ion milling. The plane view specimens were created from the top portion of the films at the surfaces where devices would be grown.

III. RESULTS AND DISCUSSION

SEM images in Figs. 1(a) and 1(b) show the microstructures of the GaN films at 3 min HT growth, prior to island coalescence. Figure 1(a) shows that for the conventional GaN grown on planar sapphire, the distribution of the GaN regions was non-uniform, and their morphology was highly irregular at this stage of growth. In contrast, the AGNP-GaN islands grown for the same time were located preferentially in the valleys between the sapphire bumps (see Fig. 1(b)), and had greater regularity in spacing, size, and geometry. These islands had distinct inclined facets that have previously been reported to correspond with significant bending of dislocations during subsequent island coalescence.[8]

In-situ reflectivity profiles of n-doped AGNP-GaN and n-doped conventional GaN growths are represented in Fig. 2 by the red solid curve (top) and blue solid curve (bottom), respectively. The two green dashed lines represent the reflectivity recovery defined as 75% of the reflectivity signal for smooth GaN,[5] which serves as a manifestation of the coalescence of GaN. The coalescence of AGNP-GaN was found to occur after 12 min of growth at HT, as marked by the two red dotted lines in Fig. 2. The AGNP-GaN thickness at this time was estimated to be 0.25 μm by considering the known growth rate.[6,7] The coalescence time was also confirmed by interrupting growth and examining the surface with SEM, as in Fig. 1. The two blue dotted lines define the etch-back and recovery (ER) processes in the conventional growth mode, indicating a coalescence time of 22 min at a GaN thickness of approximately 0.66 μm. It is important to note that the resolution limit of the reflectivity measurement is only about 500 nm, so the degree of roughness cannot be assessed with great precision at the point of coalesence. However, an extremely smooth surface is not expected in conventional GaN until later stages of growth.[8]

Cross-section TEM images of the conventional and AGNP-GaN films near the sapphire interface are shown in Figs. 3(a) and 3(b). The thicknesses of the TEM samples were different so a direct comparison of dislocation density is not readily available from the images, but variations of dislocation density within each specimen are apparent. For both samples, the interface region showed the highest dislocation density. In the conventional GaN, the dislocation density decreased steadily with increasing distance from the substrate. For example, the dislocation density was about 5 times higher in the region 2 μm from the interface than in the region 3.5 μm from the interface. In AGNP-GaN, the dislocation density underwent a dramatic reduction during the very early stages of film growth, then became quite consistent after the thickness exceeded 0.5 μm. Although some of the dislocations in both images appear to terminate before reaching the surface, actually they just exit the surface of the thin foil specimen.

A large number of dislocations in the conventional GaN were found to bend 90° (i.e., parallel to the substrate) at a
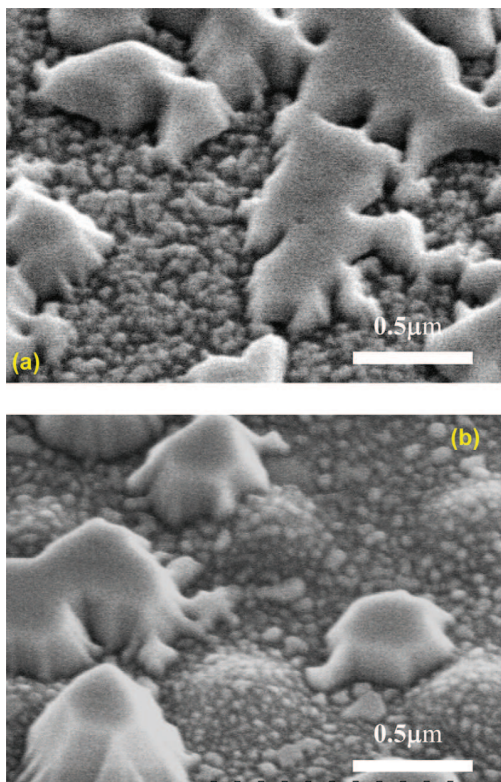

FIG. 1. (Color online) Surface morphology of (a) conventional GaN grown on planar sapphire [30 nm LT GaN and 3 min HT GaN], (b) AGNP-GaN grown on a patterned substrate [15 nm LT GaN and 3 min HT GaN].
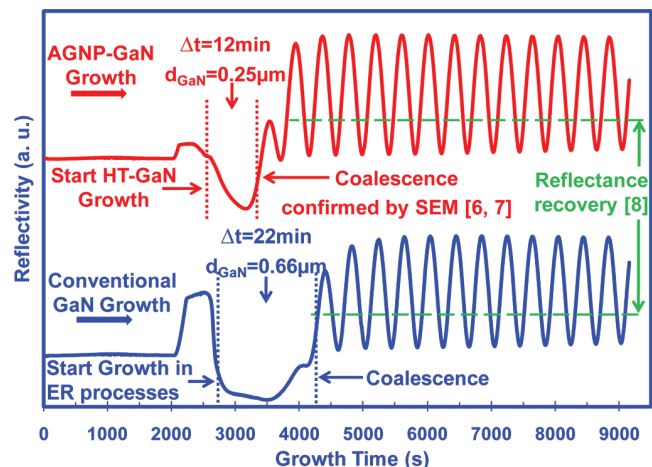

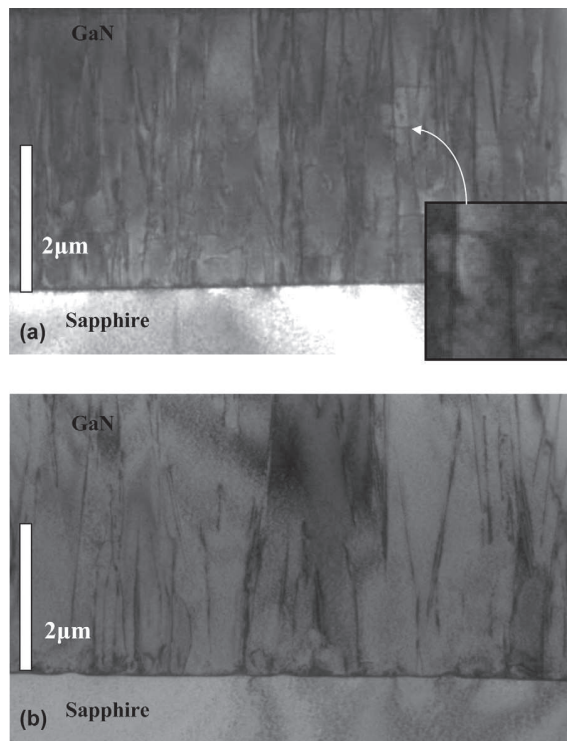FIG. 2. (Color online) Comparison of reflectivities during n-doped AGNP-GaN and conventional GaN template growth.

FIG. 3. Bright field cross-section TEM images taken at zone axis [1-210] for (a) conventional GaN, and (b) AGNP-GaN. The white arrow points to a dislocation bending 90°. The bent dislocation is also shown at greater magnification in the inset of (a).

distance from the interface of up to approximately 2.5 μm, as indicated by the white arrow and the inset in Fig. 3(a). In contrast, severe dislocation bending could be observed in the AGNP-GaN only within the region approximately 1 μm from the interface, as shown in Fig. 3(b). Dislocation bending is believed to make a major contribution to the dislocation reduction in GaN. Thus for the conventional GaN, the significant distance from the substrate interface over which bending is observed matches with the gradual dislocation density reduction that occurs over a similar distance. In the AGNP-GaN, the 90° bending was confined to a very thin layer adjacent to the interface, so most of the decrease in dislocation density occurs relatively early in the growth process.

Similar dislocation bending behavior was reported for ELO GaN samples, but only up to the point that the facetted islands coalesced and the surface became very smooth.[11,12] Reports on other types of GaN growth also suggest that dislocations cease to bend after the GaN film surface becomes smooth.[13,14] Coupled with the TEM images in Fig. 3, these findings imply that the etch-back and recovery process in our conventional GaN growth not only delayed the initial island coalescence, but also delayed surface smoothing.[8] On the other hand, the narrow band of bending dislocations in the AGNP-GaN correlates with the fast island coalescence and smooth surface morphology shown in our previous SEM study.[6,7] Once island coalescence is complete, there is little subsequent change in the dislocation density.

To obtain an accurate determination of dislocation density, bright field plane view TEM images were taken of the surface of both types of samples. The total dislocation den-

sity of both samples was about $5 \times 10^8/cm^2$ at a growth distance of approximately 4 μm. Edge, screw, and mixed dislocations were identified in plane view TEM images by their contrast differences.[15] As shown in Fig. 4, a dislocation that appears as a line without spots at its ends is of edge character. A dislocation with a line and end-spots is mixed in character, and a dislocation with end-spots but no line between them is pure screw. As summarized in Fig. 5, mixed dislocations were found to be the most dominant in the conventional GaN (60%), followed by edge dislocations (22%), and screw dislocations (18%). In the AGNP-GaN, edge dislocations were the most dominant (48%), followed by mixed (30%), and screw dislocations (22%). It has been suggested that dislocations with some screw character (i.e., pure screw and mixed) play a particularly large role in recombination,[16,17] so the substantial difference in this component between the conventional and AGNP GaN (78% versus 52%) may play a key role in the improved carrier lifetime observed previously for AGNP-GaN.[9]

The following procedure was used to determine the inclination of the dislocations to the c-axis. First, the TEM sample thickness was determined by the spot separation method, which for experimental convenience was carried out on selected screw dislocations. These dislocations were
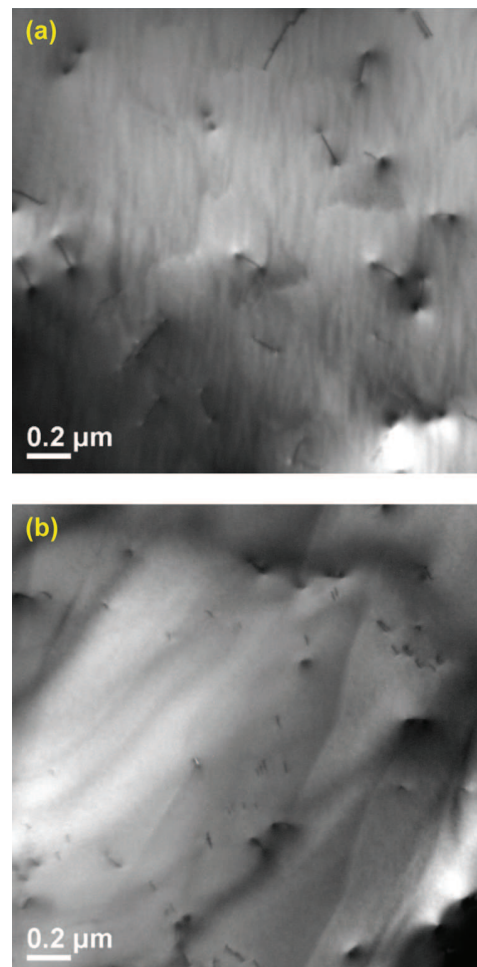

FIG. 4. (Color online) Representative bright field plane view TEM images taken at [0001] zone axis for (a) conventional GaN, and (b) AGNP-GaN.
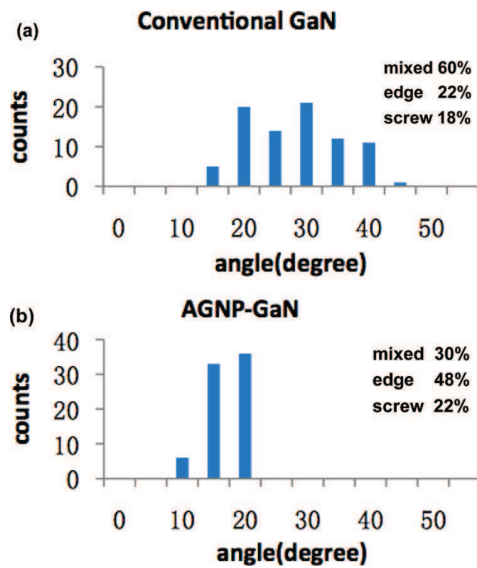
FIG. 5. (Color online) Distribution of dislocation bending angles and types for (a) conventional GaN, and (b) AGNP-GaN.

imaged at the [0001] zone axis, and the degree of specimen tilt required to superpose the spots corresponding to the intersection of the dislocation with the top and bottom surfaces, was determined. By using the simple geometric relationship between the projected length of the untilted dislocation and the tilt angle, the foil thickness values were calculated; these were found to be 220 nm and 150 nm for the conventional and AGNP GaN, respectively. The angle of inclination was then calculated for all the dislocations using measured values of the projected length and the foil thickness.

The distribution of bending angles from a number of plane view images representing a large area is summarized in Fig. 5. In the conventional GaN film, it was found that a large fraction of the dislocations near the surface are bent at a large angle between $30^{\circ} - 45^{\circ}$. In the AGNP-GaN film, however, the near-surface dislocation bending angle was found to be no more than 25°.

A $15^{\circ} - 20^{\circ}$ small angle of bending is often associated with strain relaxation during vertical film growth because this process will generate a misfit dislocation component in the basal plane and thereby help to reduce the lattice mismatch and the strain energy.[18,19] Dislocations exhibiting this degree of bending were common in both conventional and AGNP-GaN (Fig. 5). During the growth of facetted islands, line bending of threading dislocations toward the facet plane normals takes place because of image forces. This characteristic has been exploited in ELO techniques to modify the defect distribution and density.[11] The slower the coalescence and surface smoothing relative to the vertical growth rate, the greater the extent of bending that can occur. The study of dislocation bending angles by Gradečak *et al.*[12] suggested that, although the majority of edge and mixed dislocations preferentially bend at a 90° angle (because this configuration corresponds to the minimum energy), a large number of edge and mixed dislocations were found to bend $30^{\circ} - 50^{\circ}$ because of the calculated local energy minima.[12]

IV. SUMMARY

The results of the present study show that the dislocation population in the AGNP-GaN contained a significantly lower fraction of mixed dislocations than the conventional GaN, and that the degree of bending of the dislocations close to the sample surface was also less. It is suggested that these differences arise directly from the earlier coalescence and surface smoothing of the GaN islands in the AGNP case, because this limits the vertical extent of facetted island growth. Furthermore, the bending of edge dislocations introduces a screw component, which correlates with the lower proportion of mixed versus edge dislocations in the AGNP-GaN films. Note that for pure screw dislocations, the minimum energy corresponds to the straight configuration, hence the fraction at the surface is similar in both cases. These findings support earlier results showing that InGaN QW LEDs grown on nano-patterned sapphire showed enhanced output power and carrier lifetime compared with those grown on a planar template.[6,7,9] The indication also is that AGNP-GaN may achieve equivalent or better performance than conventional GaN at much smaller thickness, saving time and expense in growth.

[1] S. Nakamura, Science **281**, 956 (1998).
[2] H. Zhao, G. Liu, J. Zhang, J. D. Poplawsky, V. Dierolf, and N. Tansu, Opt. Express **19**, A991 (2011).
[3] R. M. Farrell, D. F. Feezell, M. C. Schmidt, D. A. Haeger, K. M. Kelchner, K. Iso, H. Yamada, M. Saito, K. Fujito, D. A. Cohen, J. S. Speck, S. P. DenBaars, and S. Nakamura, Jpn. J. Appl. Phys. **46**, L761 (2007).
[4] J. Zhang, H. Zhao, and N. Tansu, Appl. Phys. Lett. **97**, 111105 (2010).
[5] S. Nakamura and T. Mukai, Jpn. J. Appl. Phys. **31**, L1457 (1992).
[6] Y. K. Ee, J. M. Biser, W. Cao, H. M. Chan, R. P. Vinci, and N. Tansu, IEEE J. Sel. Top. Quantum Electron. **15**, 1066 (2009).
[7] Y. K. Ee, X. H. Li, J. E. Biser, W. Cao, H. M. Chan, R. P. Vinci, and N. Tansu, J. Cryst. Growth **312**, 1311 (2010).
[8] D. D. Koleske, A. J. Fischer, A. A. Allerman, C. C. Mitchell, K. C. Cross, S. R. Kurtz, J. J. Figiel, K. W. Fullmer, and W. G. Breiland, Appl. Phys. Lett. **81**, 1940 (2002).
[9] Y. K. Ee, X. H. Li, J. Biser, W. Cao, H. M. Chan, R. P. Vinci, and N. Tansu, (Proc. Of the IEEE/OSA Conference on Lasers and Electro-Optics (CLEO) San Jose, CA, 2010), Paper CMB2.
[10] H. Park, H. M. Chan, and R. P. Vinci, J. Mater. Res. **20**, 417 (2005).
[11] K. Hiramatsu, K. Nishiyama, M. Onishi, H. Mizutani, M. Narukawa, A. Motogaito, H. Miyake, Y. Iyechika, and K. Maeda, J. Cryst. Growth **221**, 316 (2000).
[12] S. Gradečak, P. Stadelmann, V. Wagner, and M. Ilegems, Appl. Phys. Lett. **85**, 4648 (2004).
[13] C. D. Lee, A. Sagar, R. M. Feenstra, C. K. Inoki, T. S. Kuan, W. L. Sarney, and L. Salamanca-Riba, Appl. Phys. Lett. **79**, 3428 (2001).
[14] M. J. Manfra, N. G. Weimann, J. W. P. Hsu, L. N. Pfeiffer, K. W. West, and S. N. G. Chu, Appl. Phys. Lett. **81**, 1456 (2002).
[15] D. M. Follstaedt, N. A. Missert, D. D. Koleske, C. C. Mitchell, and K. C. Cross, Appl. Phys. Lett. **83**, 4797 (2003).
[16] M. Albrecht, A. Cremades, J. Krinke, S. Christiansen, O. Ambacher, J. Piqueras, H. P. Strunk, and M. Stutzmann, Phys. Status Solidi B **216**, 409 (1999).
[17] T. Hino, S. Tomiya, T. Miyajima, K. Yanashima, S. Hashimoto, and M. Ikeda, Appl. Phys. Lett. **76**, 3421 (2000).
[18] A. E. Romanov and J. S. Speck, Appl. Phys. Lett. **83**, 2569 (2003).
[19] P. Cantu, F. Wu, P. Waltereit, S. Keller, A. E. Romanov, U. K. Mishra, S. P. Denbaars, and J. S. Speck, Appl. Phys. Lett. **83**, 674 (2003).